Observation of Stability Boundaries in the Parameter Space of Single Bubble Sonoluminescence

R. Glynn Holt and D. Felipe Gaitan

Jet Propulsion Laboratory, California Institute of Technology, Pasadena, California 91109

(Received 13 June 1996)

The region of parameter space (acoustic pressure P_a, bubble radius R_0) in which stable single bubble sonoluminescence (SBSL) occurs in an air-water system is a small fraction of that which is accessible. This is due to the existence of an island of dissolution at high P_a and small R_0. For dissolved gas concentrations above 50% of saturation, the region lies above the threshold for shape oscillations and is unobservable. Below 50%, an oscillating bubble is stabilized on the boundary of the island which lies below the shape threshold. SBSL is shown to exist exclusively along this boundary. [S0031-9007(96)01550-5]

PACS numbers: 43.25.+y, 43.35.+d, 78.60.Mq

A bubble in an external acoustic field is a laboratory for the study of a surprising variety of physics problems. Heat transport [1], mass transport [2], surfactant effects [3], shock waves [4], chaos [5], free surface instability [6], and even electromagnetic radiation [7] are all phenomena associated with the highly nonlinear oscillations of air bubbles in water. Recent observations of *stable single bubble sonoluminescence* (SBSL) have highlighted the fact that, despite the enormous amount of energy concentrated in a bubble which is emitting light, such bubble can remain both *spherically symmetric* and the *same size* over billions of oscillation cycles.

On the other hand, this behavior is far from typical. Given reasonable initial values for the pressure and frequency of the driving acoustics, bubble size, and host liquid parameters, a bubble is far more likely to dissolve and eventually disappear, or to grow and break up. Although for some cases the growth is self-limiting (see below), most of the time spherical instability will occur, and the bubble will either break up (and sometimes also disappear), or will become so large that it cannot be levitated. In fact, as discovered recently by Löfstedt *et al.* [2], stable single bubble sonoluminescence is known to occur where classical theories [2,6] predict rapid growth and subsequent destruction. The experiments described in this report represent an attempt to resolve the discrepancies between observation and model predictions. In particular, we wish to delineate where and how a bubble can exhibit both mass transport and mechanical stability by measuring where the instabilities occur for the limiting case of small bubble sizes and large acoustic pressures.

Summary of the results.—The natural parameter space for the problem is defined by the acoustic pressure P_a and the equilibrium radius R_0. The accessible range for an acoustic standing wave levitator is the minimum trapping pressure (less than 0.1 bar in 1 g, 0 in 0 g) up to about 1.5 bars. Bubbles can be stably levitated with radii ranging from less than 1 μm up to approximately 110 μm near the pressure maximum of the 20 kHz standing wave. And yet light emission from bubbles (generically SL) and the more restrictive SBSL have been observed only in a miniscule region of that space, which we loosely term the *SL window:* $1.2 \leq P_a \leq 1.4$ bars, and (less than 1) $\leq R_0 \leq 7$ μm in the current measurements at a fixed acoustic driving frequency f_a of 20.6 kHz [8].

We have discovered that SBSL occurs only on a *line path* in the space (P_a, R_0), determined by the fixed concentration of dissolved gas in the liquid; an example is the squares with positive slope in Fig. 1(c). Asymptotically stable, purely spherical bubble oscillations can occur only if they are in *mass flux equilibrium*, and then only if that equilibrium is itself stable. As we will demonstrate below, these constraints are met when the gas concentration in the liquid is below a certain value: for air in water at room temperature that threshold value is approximately 50% saturation, or equilibration at 380 mm Hg, corresponding to $C_i/C_{0L} = 0.5$, where C_i is the dissolved gas concentration in the liquid far away from the bubble, and C_0 is the concentration at equilibrium for an ambient pressure of 1 bar, and subscript "L" distinguishes this from calculated values later in the paper.

For $C_i/C_{0L} > 0.5$, bubbles are observed to obey the predictions of the Eller-Flynn [2] diffusion theory, for which Fig. 1(a) is representative. Bubbles with initial states (P_a, R_0) in the dark shaded region labeled "d" dissolve: bubbles in "g" grow until their oscillation meets the conditions for the onset of resonant, parametric shape oscillations (Faraday [9], Holt *et al.* [5]; Strube, Hullin, and Brenner *et al.* [6]), where they are no longer spherically symmetric. The boundary between growth and dissolution is labeled "EF" and represents (mostly unstable) diffusive equilibrium. The shape oscillation threshold is shown in Figs. 1(a)–1(c) as the points labeled "F". At near-SL acoustic pressures (0.8–1.4 bar), these shape oscillations lead to the breakup of the bubble. We call this repeated growth, shape oscillation, and breakup process *recycling*: To the naked eye it appears as a "dancing" or "jittering" motion as reported by numerous authors [10].

For $C_i/C_{0L} \leq 0.5$, an isolated *island of dissolution* is observed to emerge at smaller R_0 than the Faraday threshold and stabilize the recycling. In Fig. 1(a) ($C_i/C_{0L} = 0.5$) the island just intersects F at (1.2 bar, 7 μm); only

this bubble is spherically stable, and light emission begins precisely here. At increasingly lower gas concentrations [Figs. 1(b) and 1(c)], the island extends to lower R_0, and covers a larger range of P_a at its intersection with the Faraday threshold. Bubbles (emitting light or not) are observed to be in *stable* mass flux equilibrium on the boundary of this island. Stable equilibrium requires that a bubble move from a growth regime to a dissolution regime as R_0 is increasing, and vice versa. Thus the left side of the boundary is a growth region, and the right side is a dissolution region.

SL occurs in bubbles on this boundary, and only bubbles on this boundary satisfy the condition for SBSL. However, this stable mass equilibration is neither *sufficient* nor *necessary* for light emission. For example, in Fig. 1(c) light is first emitted at the point on the upper segment of the boundary marked by the arrow. No light is emitted by the mechanically and mass flux stable bubbles on the lower segment. In Fig. 1(a), light is observed for recycling bubbles continuously along the boundary F for $1.26 \leq P_a \leq 1.4$ [11]. Recycling bubbles are clearly not in dynamic mass equilibrium, diffusive or otherwise, nor are they in mechanical equilibrium. Thus the light emission mechanism is not slaved to the mechanism for mass equilibration. The importance of the dissolution island is in providing a stable path into an area of parameter space not other wise accessible (except transiently), and making stable *periodic* SL (thus SBSL) possible. Our results complement the observations of the UCLA group [12].

Description of the measurements and techniques.— Air bubbles initiated via electrolysis are acoustically levitated in water in the 20 kHz standing wave field of a nearly closed cylindrical resonance cell ([13], Gaitan *et al.* [7]). The acoustic pressure P_a at the antinode is obtained from a custom hydrophone mounted inside the cell. R_0, $R_{\max}$, and $R_{\min}$, deviations from sphericity and translations of the bubble are obtained from single frame video images illuminated stroboscopically; R_0, in particular, is obtained by turning the sound field off instantaneously. $R(t)$ is obtained by calibrating the intensity $I(t)$ scattered into a PMT located at 80° from the forward of an incident He-Ne laser [14]. $I(t)$ is also used to detect the onset and frequency of shape oscillations. Dissolved gas concentrations less than saturation are obtained by allowing the water to equilibrate at a reduced pressure; C_i/C_{0L} is inferred using Henry's law.

We report here only those measurements for $R_0 \leq 20\ \mu$m, and $P_a \geq 0.6$ bar, and restrict ourselves to dissolved gas content $0.1 \leq C_i/C_{0L} \leq 0.5$

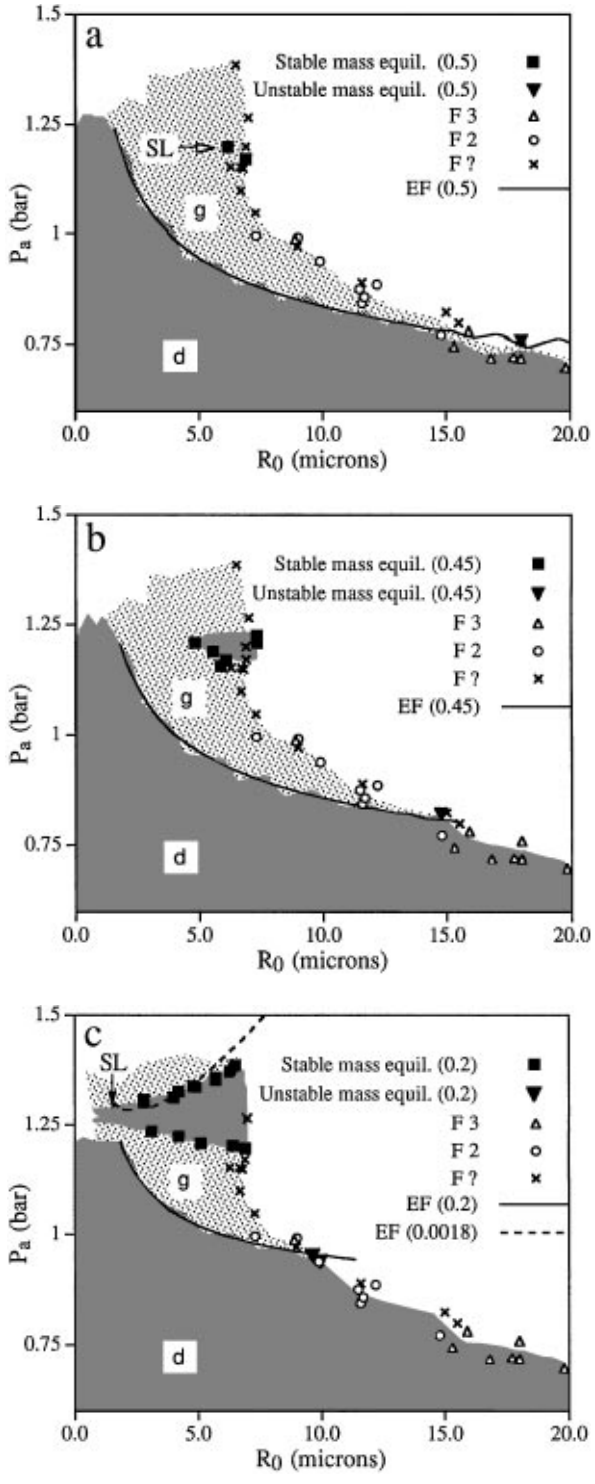

FIG. 1. Surfaces of constant dissolved air concentration from the 3D parameter space $(P_a, R_0, C_i/C_0)$ for acoustically levitated air bubbles in pure water. All bubbles are levitated in a cylindrical cell at 20.6 kHz. The symbols labeled "F n" are the measured values (P_a, R_0) at the onset of the Faraday instability for the nth mode ("?" indicates mode was undetermined). The line labeled "EF (C_i/C_0)" is the numerically generated diffusional equilibrium (1) for the experimentally measured C_i/C_{0L} using an RP equation [18]. The solid points are the measured mass flux equilibria at the given concentration: squares are stable, inverted triangles are unstable. Bubbles are observed to grow in regions labeled "g"; to dissolve in dark shaded regions labeled "d". (a) $C_i/C_{0L} \approx 0.5$; (b) $C_i/C_{0L} \approx 0.45$; (c) $C_i/C_{0L} \approx 0.2$; the arrow labeled "SL" indicates the minimum (P_a, R_0) where light is first emitted. (c) additionally displays the calculation of the Eller-Flynn equilibrium for $C_i/C_0 = 0.0018$ for comparison with the island boundary points on the upper segment.

[15]. Points F are measured by varying C_i/C_{0L} over many values, since it is practical to measure the point at which *unstable* mass equilibrium and the threshold for the onset of shape oscillations intersect. The threshold F is invariant with respect to changes in C_i/C_{0L}. A typical run at fixed C_i/C_{0L} begins at the EF-F intersection, which is the first mass flux equilibrium encountered as P_a is increased. We then increase P_a, and the bubble remains near F because it is recycling. At $P_a = 1.2$ bar (for suitably low C_i/C_{0L}), we encounter the *stable* mass equilibrium regime: the lower boundary of the dissolution island. Increasing P_a, we measure spherically symmetric bubble oscillations along this asymptotically stable boundary, which takes us rapidly to smaller R_0, then back again; see the squares in Fig. 1(c), for example. P_a is increased until F is reached again, or the bubble disappears, or both.

Faraday instability.—Only the spherically symmetric volume mode is directly forced by the time-varying acoustic pressure. Under what conditions will this spherical symmetry become unstable, and lead to observable distortions of the shape and eventual breakup of the bubble?

Our observations show that, for all P_a below 1.4 bars, the instability which develops first is the Faraday instability. Figure 1 shows the measured threshold as a series of points labeled "F n," that is, the onset of normal shape modal oscillations of observed mode n. The crucial observation which distinguishes this instability from the Rayleigh-Taylor instability [16] is that the normal mode couples resonantly to the nearly periodic ringing oscillation. Thus we see the shape mode and subsequent breakup occur 2 or more collapses *after* the first (light-producing) collapse. Brenner *et al.* [6] have presented detailed calculations of the onset of only the quadrupole mode nonlinearly coupled to the volume mode. The numerically generated threshold agrees very well with our measurements until above 1 bar. The *internal resonance* condition $f_n{:}f_0 \cong 1{:}2$ (where f_n is the Lamb [17] frequency for the observed mode and liquid parameters, and f_0 is the linear volume mode resonance frequency for the observed R_0) is verified for all the modes we observe for $R_0 \leq 20$ μm.

Mass flux equilibrium: observations, mechanisms, stability.—Our observations show that in the subspace of purely spherical oscillations (to the left of F), there exist two apparently disconnected regions of dissolution for $0.2 \leq C_i/C_{0L} \leq 0.5$. These regions are denoted by dark shading and labeled as "d" in Figs. 1(a)–1(c). The rest of the accessible space is labeled "g" for growth. Thus we observe two disconnected sets of mass flux equilibria at the boundaries of these regions. The lower equilibrium is unstable; the two upper equilibria are stable.

Eller and Flynn [2] showed that the net effect of oscillations was to enhance *diffusive* transport of dissolved gas into the bubble. For large enough amplitude oscillations for a fixed C_i, this "rectified diffusion" could balance the natural dissolution of a bubble in an undersaturated solution. The dynamic diffusion equilibrium they derive using a boundary layer approximation is

$$\frac{C_i}{C_0} = \left(1 + \frac{2\sigma}{R_0 P_\infty}\right) \frac{\langle R/R_0 \rangle}{\langle (R/R_0)^4 \rangle}, \tag{1}$$

where σ is the liquid surface tension, P_∞ is the ambient pressure outside the liquid, and $\langle \cdots \rangle$ denotes the time average of the quantity over one acoustic cycle. The curves EF in Figs. 1(a)–1(c) represent numerically generated (P_a, R_0) values where an oscillating bubble is in diffusion equilibrium for numerical $C_i/C_0 = C_i/C_{0L}$, using $R(t)$ calculated from a Rayleigh-Plesset model [18]. For example, in Fig. 1(a) EF (0.5) represents the condition $C_i/C_0 = 0.5$. For the region (P_a, R_0) above and to the right of EF the model predicts diffusive growth; below left it predicts dissolution. This agrees with our observations for $C_i/C_0 = 0.5$. The wiggles in the curve EF (0.50) in Fig. 1(a) are due to underlying harmonic resonances [19]. EF curves with positive slope are stable equilibria—negative slopes are unstable. Brenner *et al.* [2] have suggested that the intermittent stable regions such as seen on EF (0.5) in Fig. 1(a) could be responsible for stable SL; while in practice resonances are important at larger bubble size [13,15], our measurements show that harmonic volume resonance effects are not important in the SL window in water.

EF intersects F very near where our unstable mass equilibria intersect F in Figs. 1(a)–1(c), indicating that our unstable mass equilibria are in diffusive equilibrium. However, (1) predicts a single connected [and mostly unstable for these (P_a, R_0) values] equilibrium line, with a continuous region of growth above and to the right. The Eller-Flynn theory fails to predict our observations of stable mass flux equilibria in the SL window for $C_i/C_{0L} < 0.5$.

We can substitute our *measured* bubble response $R(t)$ into (1) to further investigate the nature of the equilibria. Figure 2 plots $C_i/C_{0\,(\mathrm{Eq.(1)})}$ for every bubble in mass flux equilibrium for two similar C_i/C_{0L}. The unstable equilibrium data obey EF diffusion; that is, for a given water preparation, we find $C_i/C_{0\,(\mathrm{Eq.(1)})} = C_i/C_{0L}$ for the spherical bubble at the EF-F intersection. However, for stable bubbles along the island boundary, we find $C_i/C_{0\,(\mathrm{Eq.(1)})} \ll C_i/C_{0L}$, falling while traversing the lower segment to reach a value 2 orders of magnitude lower than the preparation value. Such bubbles are not in diffusive equilibrium with air, at least not in the EF formulation with air treated as a lumped mixture with constant properties. This is in agreement with the observations of Barber *et al.* [8] and Löfstedt *et al.* [2]; they report an air bubble with roughly the same $P_a, R_0, R_{\max}$ which does not satisfy an approximate expression derived from (1).

Strikingly, the bubble response along the upper segment of the island boundary yields a constant (0.0018) value for $C_i/C_{0\,(\mathrm{Eq.(1)})}$. This is consistent with the fact that both $R_{\max}$ and R_0 are increasing, and their opposite effects on the dynamic mass flux just balance each other. Figure 1(c) displays the fully numerical diffusion

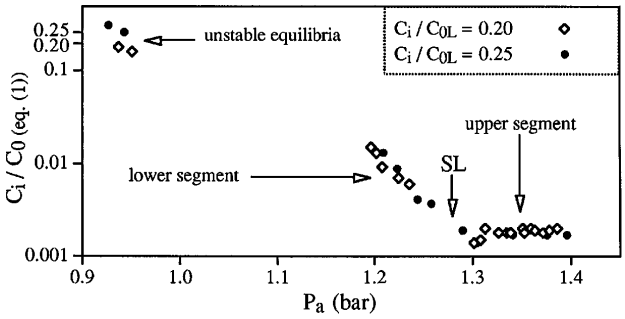

FIG. 2. Dissolved gas concentration $C_i/C_{0\,(\mathrm{Eq.(1)})}$ calculated from (1) using the measured $R(t)$ for the stable and unstable mass flux equilibria vs acoustic pressure P_a for two data sets. The inferred C_i/C_{0L} from Henry's law is constant for each data set and drawn on the axis.

equilibrium from Eq. (1) for $C_i/C_0 = 0.0018$ for comparison. Bubbles on the upper segment may well be in stable diffusional equilibrium for some reduced "effective gas concentration" just outside the bubble. Differential (or preferential) diffusion of component gases may also play a role here. Recently Lohse *et al.* [20] have suggested a nitrogen dissociation mechanism which could account for such behavior. Their parameter space calculations (Hilgenfeldt *et al.* [20]) show remarkable qualitative agreement with our results here. Whatever the mass stabilization mechanism is, we can now quantify its constraint on values of (P_a, R_0) on the upper island boundary: Equation (1) is a constant of the motion.

We have observed mechanical stability and mass transport boundaries in the parameter space of an acoustically levitated bubble which determine its behavior. The Faraday instability limits the maximum equilibrium size of spherically oscillating bubbles at a fixed pressure, while dynamic mass flux equilibrium constrains the size of the bubble at fixed pressure such that it remains along a stable, zero-mass-flux path. This constraint yields very high values of bubble response, and thus provides a window in state space in which SBSL appears. The key observation is the existence of the dissolution island (which stabilizes spherical oscillations relative to the Faraday instability) and its dependence on the dissolved gas concentration.

We gratefully acknowledge support from NASA MSAD, the JPL/Caltech Supercomputing Fund, discussions with J. Holzfuss, R. Roy, and the use of equipment loaned to us by E. Trinh.

[1] M. S. Plesset and S. A. Zwick, J. Appl. Phys. **23**, 95 (1952); K. Yasui, J. Acoust. Soc. Am. **98**, 2772 (1995).

[2] A. Eller and H. G. Flynn, J. Acoust. Soc. Am. **37**, 493 (1965); R. K. Gould, J. Acoust. Soc. Am. **56**, 1740 (1974); C. C. Church, J. Acoust. Soc. Am. **83**, 2210 (1988); M. M. Fyrillas and A. J. Szeri, J. Fluid Mech. **277**, 381 (1994); R. Löfstedt *et al.,* Phys. Rev. E **51**, 4400 (1995); M. P. Brenner *et al.,* Phys. Rev. Lett. **76**, 1158 (1996).

[3] L. A. Crum, J. Acoust. Soc. Am. **68**, 203 (1980); D. O. Johnson and K. J. Stebe, J. Colloid Interface Sci. **168**, 21 (1994); M. M. Fyrillas and A. J. Szeri, J. Fluid Mech. **289**, 295 (1995).

[4] R. Hickling and M. S. Plesset, Phys. Fluids **7**, 7 (1964); C. C. Wu and P. H. Roberts, Phys. Rev. Lett. **70**, 3424 (1993).

[5] R. G. Holt *et al., Proceedings of the 12th International Symposium on Nonlinear Acoustics, Austin, Texas,* edited by M. F. Hamilton and D. T. Blackstock (Elsevier, New York, 1990), p. 497; R. G. Holt *et al.,* Phys. Rev. Lett. **72**, 1376 (1994).

[6] G. Birkhoff, Q. Appl. Mech. **12**, 306 (1954); **13**, 451 (1956); A. I. Eller and L. A. Crum, J. Acoust. Soc. Am. **47**, 762 (1970); H. W. Strube, Acustica **25**, 289 (1971); C. Hullin, Acustica **37**, 64 (1977); M. P. Brenner *et al.,* Phys. Rev. Lett. **75**, 954 (1995).

[7] N. Marinesco and J. J. Trillat, Proc. R. Acad. Sci. **196**, 858 (1933); D. F. Gaitan *et al.,* J. Acoust. Soc. Am **91**, 3166 (1992); B. P. Barber and S. J. Putterman, Nature (London) **352**, 318 (1991); B. P. Barber *et al.,* Phys. Rev. Lett. **74**, 5276 (1995).

[8] There is rough agreement among experimental groups, and the differences are due in the main to (1) different acoustic frequencies, and (2) the methods utilized for either inferring P_a and R_0 from light scattering [B. P. Barber *et al.,* Phys. Rev. Lett. **72**, 1380 (1994); R. Löfstedt *et al.,* in Ref. [2] or calibrating P_a and R_0 measurements (this work; D. F. Gaitan, Ph.D. thesis, University of Mississippi, 1990; S. M. Cordry, Ph.D. thesis, University of Mississippi, 1995; T. R. Stottlemyer, Ph.D. thesis, Yale University, 1996).

[9] M. Faraday, Philos. Trans. R. Soc. London **121**, 299 (1831).

[10] This source of "dancing" translations [Barber *et al.,* Löfstedt *et al.,* in Ref. [8], K. Weninger *et al.,* J. Phys. Chem. **99**, 14 195 (1995)] should be distinguished from another shape-oscillation phenomenon, *self-propulsion* due to coupling between shape modes [see Eller and Crum, in Ref. [6]; T. B. Benjamin and A. T. Ellis, J. Fluid Mech. **212**, 65 (1990); Z. C. Feng and L. G. Leal, Phys. Fluids **7**, 1325 (1995).

[11] As did Gaitan *et al.,* in Ref. [7], their Figs. 20 and 21, and later Barber *et al.* in Ref. [7], their Fig. 4, they have used the term "unstable SL" to refer to the light emission by recycling bubbles.

[12] Figure 2 in Barber *et al.,* in Ref. [8]; Figs. 1, 8, 11, and 12 in Löfstedt *et al.,* in Ref. [2], where different combinations of gas are used, but always at total gas partial pressure near 150 Torr.

[13] R. G. Holt and L. A. Crum, J. Acoust. Soc. Am. **91**, 1924 (1992).

[14] R. G. Holt and L. A. Crum, Appl. Opt. **29**, 4182 (1990).

[15] R. G. Holt and D. F. Gaitan, APS Bull. **40**, 1960 (1995).

[16] G. I. Taylor, Proc. R. Soc. London A **201**, 192 (1950); M. S. Plesset, J. Appl. Phys. **25**, 96 (1954).

[17] H. Lamb, *Hydrodynamics* (Dover, New York, 1945).

[18] A. Prosperetti *et al.,* J. Acoust. Soc. Am. **83**, 502 (1988).

[19] U. Parlitz *et al.,* J. Acoust. Soc. Am. **88**, 1061 (1990); C. C. Church in Ref. [2].

[20] D. Lohse *et al.* (to be published); S. Hilgenfeldt *et al.,* Phys. Fluids (to be published).